Statistical theory of mixtures with surfactants

Wojciech T. Góźdź

January 1996

ACKNOWLEDGMENTS

I would like to express my gratitude to my adviser, doc. dr hab. Robert Hołyst, for his sincere interest in, and support of my work. I would like to express my special thanks to Professor Jan Stecki, whose influence on my professional life has been enormous, although indirect. My MSc thesis advisor, Professor Stefan Sokołowski, and my PhD advisor have done their PhD under supervision of Professor Stecki. It has been pleasure to me to work on my PhD thesis in the department, whose head is Professor Stecki. I have met there many people, with whom I enjoyed discussing, arguing, and socializing. I will remember for a long time discussions with: doc. dr hab. A. Ciach, dr. A. Maciołek, dr E. Naumowicz-Węglinska, dr hab. A. Poniewierski, dr A. Samborski, dr S. Wieczorek, dr A. Żywociński.

The calculations have been done on the computers sponsored by Fundacja Współpracy Polsko-Niemieckiej.

This work was supported by Komitet Badań Naukowych.

Contents

List of Figures

List of Tables

Chapter 1

Introduction: What is a microemulsion ?

Amphiphilic molecules are composed of two different parts: hydrophobic tail and hydrophilic head. An example of an amphiphilic molecule is shown in Fig. 1.1. The tail is composed of one or more hydrocarbon chains, usually with 6 to 20 carbon atoms, the head is composed of chemical groups of high affinity to water [1, 2]. Such a composition of amphiphilic molecules results in many amazing properties of systems containing these molecules. Adding an appropriate amount of amphiphile to a mixture of oil and water, two liquids which are immiscible under normal conditions, causes complete mixing of these liquids. The amount of amphiphile necessary to cause mixing depends on the strength of amphiphile. The longer the hydrocarbon chain the stronger the amphiphile is. The strength of amphiphile depends in similar way on the number of hydrophilic groups in the amphiphilic molecule. Complete mixing

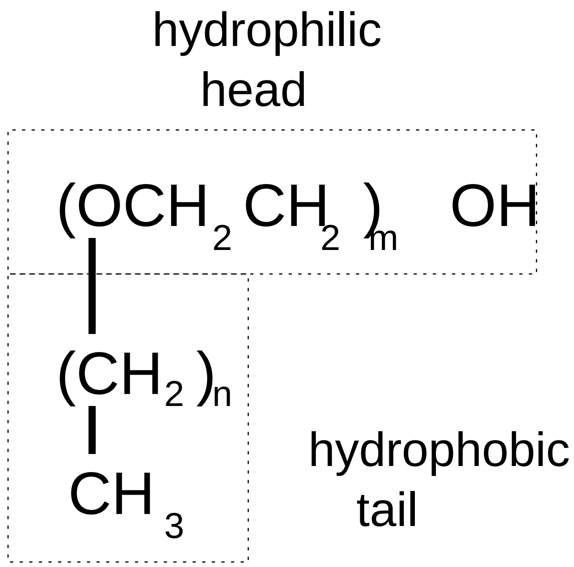

Figure 1.1: A non-ionic surfactant C_nE_m. Alkylpolyoxyethylen

is enabled by lowering the oil-water surface tension by amphiphile. That is why the amphiphilic molecules are also called surfactants: surface active agents. The surfactant assembles at the interface, forming a monolayer, in such a way that the hydrophilic part of the amphiphile is located in water and hydrophobic part in oil. The surfactant monolayer separates coherent regions of oil and water. Usually the monolayer width is small compared to the size of oil and water regions, unless the concentration of surfactant is very high. In such a situation the formation of water and oil droplets suspended in the surfactant solution is possible. Surfactants dissolved in water can form micells of different shape: spherical or cylindrical. They can also assemble into bilayers grouping the hydrophobic part of the surfactant inside the bilayer. Such system is called the sponge phase.

When comparable amount of oil and water are mixed with surfactant a new homogeneous, isotropic, thermodynamically stable phase is created [3]. This phase, called microemulsion, can coexist with oil and water [4, 1, 2]. The measurements of electrical conductivity, self diffusion, NMR and freeze fracture microscopy studies indicate that the structure of microemulsion is bicontinuous [5, 6, 1, 7, 8]. That is the microemulsion is composed of water and oil channels mutually interwoven, separated by the monolayer of surfactant. The description of microemulsion structure is a challenge for modern condensed matter physics.

The amphiphilic systems can form apart from the structured disordered phase like microemulsion, many ordered phases. The most common are the lamellar and hexagonal. The lamellar phase is composed of the regions of water and oil separated by the surfactant monolayer. The lamellar phase looks like a sandwich composed of the slices of water and oil separated by a monolayer of surfactant. The hexagonal phase is composed of cylinders of water or oil bounded by the layer of surfactant, arranged on a hexagonal lattice, immersed in oil or water. The most interesting are the ordered cubic bicontinuous phases. The most prominent examples are the gyroid, double diamond (sometimes called diamond), and simple cubic phase. Although the structure of a bicontinuous phase on a mesoscopic scale is difficult to study experimentally, the experimental methods like freeze fracture microscopy or x-ray and neutron scattering revealed some details. In the scattering experiments one is able to study the symmetry, the freeze fracture microscopy gives some information about the topology.

The systems containing surfactants are difficult to characterize. They are structured liquid ternary mixtures. For example microemulsion on a macroscopic level looks like an ordinary, homogeneous fluid. However, it is known that the microemulsion is composed of three components: two of them, oil and water do not mix in the absence of the third one, the surfactant. Thus the presence of the surfactant is crucial. It is obvious that information about the location of surfactant in its mixtures characterizes the mixtures in the best way. **The surfactant forms a monolayer at the water-oil interface. This monolayer can be approximated in the theory by a mathematical surface. Thus in order to characterize the systems containing surfactants it is enough to characterize this surface and its properties such as the surface area, genus and its curvatures** [9, 10, 11, 12, 13].

There are three levels of description of these mixtures: macroscopic, mesoscopic, and microscopic. Here we concentrate on the mesoscopic level, described by the Landau-Ginzburg theory developed recently. We note that the most interesting phenomena take place on the mesoscopic scale, that is intermediate between the microscopic and macroscopic. The typical sizes of oil-rich domains in the mixture are often of the size of 1000Å, a size much larger than the size of a surfactant (25Å), but much smaller than the macroscopic scale of millimeters [1]. **It means that microemulsion is structured on the mesoscopic scale and that fact justifies the choice of the Landau-Ginzburg model for its descriptions.** In the next section we describe the Landau-Ginzburg theory that we use to generate the surfaces in the oil, water, surfactant mixtures.

Chapter 2

Landau-Ginzburg model

The theoretical model describing the behavior of the system containing surfactants originates form the expansion in gradients of the Landau-Ginzburg free energy [14]:

$$
\begin{aligned}
\mathcal{F}[\phi(\mathbf{r})] = \int d^3\mathbf{r}\Big(&a_0 + a_1\phi(\mathbf{r}) + a_2\phi(\mathbf{r})^2 + a_3\phi(\mathbf{r})^3 + a_4\phi(\mathbf{r})^4 \\
&+ a_5\phi(\mathbf{r})^5 + a_6\phi(\mathbf{r})^6 + \cdots \\
&+ c_1 \mid \nabla\phi(\mathbf{r}) \mid^2 + c_2 \mid \triangle\phi(\mathbf{r}) \mid^2 + \cdots \\
&+ \phi(\mathbf{r})^2 \mid \nabla\phi(\mathbf{r}) \mid^2 + \cdots \Big).
\end{aligned}
\tag{2.1}
$$

This is the simplest model with a single scalar order parameter $\phi(\mathbf{r})$. The analysis of (2.1) shows that the essential features of systems with internal interfaces can be recovered by keeping $c_1 < 0$ and $c_2 > 0$. The gradient term with negative coefficient c_1 tends to create the interface, whereas the laplacian term with the positive coefficient c_2 stabilizes the system. The number of terms and the values of coefficients, in the expansion of the scalar order parameter $\phi(\mathbf{r})$ in power series, depends on the problem to be studied. In order to study microemulsion and ordered phases which appear in systems containing surfactants the following Landau-Ginzburg functional was proposed [15, 16] based on (2.1)

$$\begin{aligned}\mathcal{F}\left[\phi(\mathbf{r})\right] = \int d^3\mathbf{r}\Big(c \mid \triangle\phi(\mathbf{r}) \mid^2 + g\left[\phi(\mathbf{r})\right] \mid \nabla\phi(\mathbf{r}) \mid^2 \\ + f\left[\phi(\mathbf{r})\right] + \mu\phi(\mathbf{r})\Big).\end{aligned} \tag{2.2}$$

The values of the field $\phi(\mathbf{r})$ are proportional to the difference in oil and water concentrations and are negative for water and positive for oil region or vice versa. The sign is just the matter of convention. The surface

$$\phi(\mathbf{r}) = 0 \tag{2.3}$$

describes the interface between oil and water. The function $f[\phi(\mathbf{r})]$ is the bulk free energy. μ is the chemical potential difference between oil and water. The surfactant degrees of freedom are considered as being integrated out and the surfactant properties enter the functional (2.2) through the form of the functions $g[\phi(\mathbf{r})]$ and $f[\phi(\mathbf{r})]$. The functional (2.2) can be also used to model the sponge phase. In such a case the negative values of order parameter are interpreted as the interior part of the sponge phase and positive as exterior part of the phase (or vice versa).

The thermodynamic quantities and correlation functions can be obtained from (2.2) by functional integration. The two point correlation function is given by

$$< \phi(\mathbf{r_1})\phi(\mathbf{r_2}) >= \frac{\int D\{\phi(\mathbf{r})\}\phi(\mathbf{r_1})\phi(\mathbf{r_2}) \exp\{-\mathcal{F}[\phi(\mathbf{r})]\}}{\int D\{\phi(\mathbf{r})\} \exp\{-\mathcal{F}[\phi(\mathbf{r})]\}}. \tag{2.4}$$

The functional integration cannot be usually performed exactly. One has to use some approximation method to evaluate the functional integral. The most often used is mean-field approximation, in which the integral is replaced with the maximum of the integrand, i.e. one has to find the minimum of $\mathcal{F}[\phi(\mathbf{r})]$, which satisfy the mean-field equation

$$\frac{\delta \mathcal{F}[\phi(\mathbf{r})]}{\delta \phi(\mathbf{r})} = 0. \tag{2.5}$$

In the Gaussian approximation the water-water structure factor $S_{ww}(k)$ (Fourier transform of the correlation function (2.4)) for (2.2) is given by

$$S_{ww}(k) \propto \frac{1}{ck^4 + g(\phi_b)k^2 + \frac{1}{2}f''(\phi_b)}, \tag{2.6}$$

$\phi_b \in \{\phi_w, \phi_m, \phi_o\}$, and for oil-rich phase $< \phi(\mathbf{r}) >\simeq \phi_o$, for water-rich phase $< \phi(\mathbf{r}) >\simeq \phi_w$, for microemulsion $< \phi(\mathbf{r}) >\simeq \phi_m = 0$. A peak at $k > 0$ (for $\phi_b = \phi_m$) indicates a local structure of microemulsion with characteristic size

$\xi \sim \frac{2\pi}{k}$. For $\phi_b = \phi_o$ or ϕ_w the structure factor has a peak only at $k = 0$ indicating that pure oil and water phase behaves like normal liquid with no internal structure. The water-water structure factor $S_{ww}(k)$ can be measured in experiments. Thus the quality of the theory can be checked out by comparing theoretical predictions with an experiment. It turns out that (2.6) describes extremally well the data from the scattering experiments [15, 7]. The model (2.2) has been successfully used to describe wetting behavior of the microemulsion at the oil-water interface [16, 17, 18, 19], to investigate a few ordered phases such as lamellar, double diamond, simple cubic, hexagonal or crystals of spherical micells [20, 21], and to study the mixtures cotaining surfactant in confined geometry [22] .

An enormous advantage of the model (2.2) is its simplicity. It is extraordinary that the properties of a very complex system are described by the one scalar order parameter field. There are a few Landau-Ginzburg theories with more than one order parameter field [5, 23, 24, 25, 26, 27]. However, adding a new order parameter field does not automatically make the model better. It does, for sure, make solving the model more difficult and it involves introduction of new parameters, physical meaning of which is not always clear.

We have used in our calculations the model (2.2) with the functions $g[\phi(\mathbf{r})]$, $f[\phi(\mathbf{r})]$ given by

$$g\left[\phi(\mathbf{r})\right] = g_2\phi(\mathbf{r})^2 + g_0, \tag{2.7}$$

$$f\left[\phi(\mathbf{r})\right] = \omega\Big(\phi(\mathbf{r}) + \phi_w\Big)^2\Big(\phi(\mathbf{r})^2 + f_0\Big)\Big(\phi(\mathbf{r}) + \phi_o\Big)^2 \tag{2.8}$$

and following set of constants: $\phi_o = -\phi_w = 1$, $c = 1$, $\omega = 1$, $\mu = 0$. Thus the functional (2.2) takes the form

$$\begin{aligned}\mathcal{F}[\phi(\mathbf{r})] = \int d^3\mathbf{r}\Big(&\mid \triangle\phi(\mathbf{r}) \mid^2 + (g_2\phi(\mathbf{r})^2 + g_0) \mid \nabla\phi(\mathbf{r}) \mid^2 \\ &+ (\phi(\mathbf{r})^2 - 1)^2(\phi(\mathbf{r})^2 + f_0)\Big).\end{aligned} \tag{2.9}$$

The function $f[\phi(\mathbf{r})]$ has by construction three minima, which guarantees three phase coexistence, i.e. oil, water, and microemulsion. The minima for oil-rich and water-rich phase are of equal depth, which makes the system symmetric, therefore μ has to be set to zero. Varying the parameter f_0 makes the middle phase (microemulsion) more or less stable with respect to two bulk phases. Thus f_0 is proportional to the chemical potential of microemulsion. The constant g_2 depends on g_0 and f_0 and is chosen in such a way that the correlation function $G(r) =< \phi(\mathbf{r})\phi(\mathbf{0}) >$ decays monotonically in the oil-rich and water-rich phases. Here we take $g_2 = 4\sqrt{1+f_0} - g_0 + 0.01$. The more negative g_0 the stronger or the more surfactant is used.

In the mean-field approximation the stable or metastable phases of the system correspond to the minimum of the functional (2.2). Finding the minima of the functional (2.2) is not a trivial task. There are not known analytic methods to deal with such problems. In the case of bicontinuous phases two methods have been used with some success. The first is expansion of the order parameter in a Fourier series, the second is Monte Carlo simulation.

The Fourier series approach was used by Gompper and Zschocke [21]. They expanded the order parameter $\phi(\mathbf{r})$ in the following way:

$$\phi(\mathbf{r}) = \sum_{i=0}^{N} \sum_{\mathbf{K} \in B_i} \phi_{\mathbf{K}} \cos(\mathbf{K} \cdot \mathbf{r}), \tag{2.10}$$

where sum runs over all reciprocal lattice vectors of a given lattice structure, B_i denotes the ith shell of the reciprocal lattice. Such approach has a few disadvantages. One has to know a priori how the solution looks like to be able to construct the Fourier series. The quality of the Fourier expansion is not know, because it is difficult to say in advance how many shells have to be taken to approximate well the investigated structures. Moreover the number of shells taken in the approximation is limited, because the more shells are taken the more variables have to be minimized.

The Monte Carlo method, used by Gompper and Kraus [28] seems to be an ideal solutions. However, it also has some disadvantages. The continuous model has to be discretized. The quality of discretization depends on the size of the lattice which is limited by the speed of computers and the computer memory. Due to the fluctuations, taken into account in simulations, the local properties of the functional, as e.g. the shape of the interface given by $\phi(\mathbf{r}) = 0$, cannot be described with sufficient accuracy.

The method we propose is a new one. It requires the discretization of a continuous model as in the Monte Carlo simulations, but the local properties of the structures can be computed with very high accuracy. Moreover the topology of the investigated structures does not have to be known in advance. This is enormous advantage of the method, as our results show it would be very hard to imagine the topology of many structures discovered by us.

As we have noticed in the Introduction the crucial information about the structure are contained in the properties of the surface $\phi(\mathbf{r}) = 0$ formed, in the system, by surfactant. We have observed [29] the very special property of the functional (2.9) related to this surface. We have discovered it by analyzing the formula for the mean curvature expressed in terms of the three dimensional field $\phi(\mathbf{r})$. From the form of (2.9) one can realize that indeed for some local minima of (2.9) the average curvature given by

$$H(\mathbf{r}) = -\frac{1}{2}\nabla\left(\frac{\nabla\phi(\mathbf{r})}{|\nabla\phi(\mathbf{r})|}\right) = -\frac{1}{2}\frac{\triangle\phi(\mathbf{r})}{|\nabla\phi(\mathbf{r})|} + \frac{\nabla\phi(\mathbf{r})\nabla|\nabla\phi(\mathbf{r})|}{2|\nabla\phi(\mathbf{r})|^2} \qquad (2.11)$$

vanishes at every point of the $\phi(\mathbf{r}) = 0$ surface. It follows from the second term of (2.9) that $|\nabla\phi(\mathbf{r})|$ should have the maximal value for $\phi(\mathbf{r}) = 0$ (note that $g_0 < 0$) and consequently the second term (which after a small algebra can be written as $(\partial|\nabla\phi(\mathbf{r})|/\partial n)/2|\nabla\phi(\mathbf{r})|$, with ∂n denoting the derivative along the normal to the surface) in (2.11) vanishes. Also for the $\phi(\mathbf{r})$, $-\phi(\mathbf{r})$ symmetry we know that $H(\mathbf{r})$ averaged over the whole surface should be zero. It means that either $\triangle\phi(\mathbf{r})$ is exactly zero at the surface or it changes sign. From the first term of (2.9) it follows that the former is favored and consequently $H(\mathbf{r}) = 0$ at every point $\mathbf{r}$ at the surface $\phi(\mathbf{r}) = 0$. The surface such that the mean curvature vanishes at its every point is called minimal, Fig. 2.1 . Therefore before solving (2.9) we observe that among the local minima of the functional (2.9) the structures with minimal surfaces should be favored.

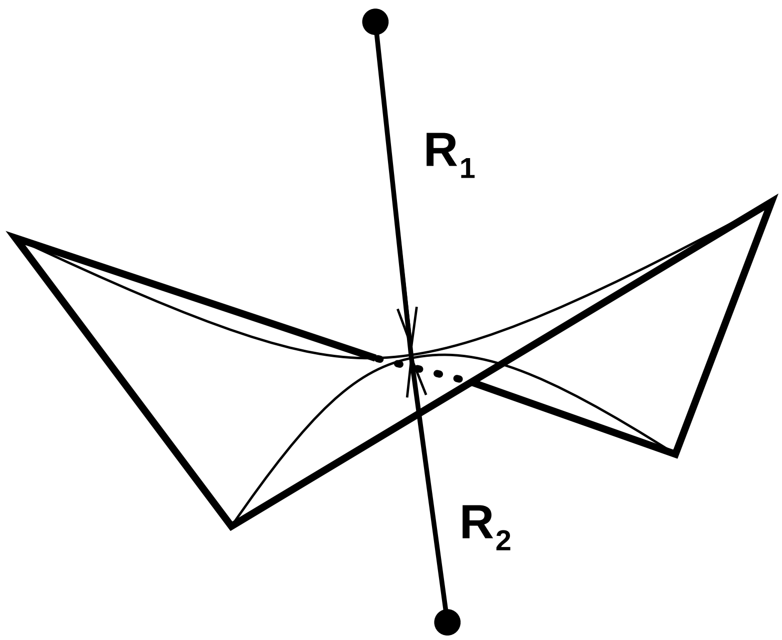

Figure 2.1: The figure illustrates a piece of surface with non-positive Gaussian curvature. R_1 and R_2 are the principal radii. The Gaussian (K) and the mean (H) curvatures are expressed in terms of the principal radii as follows: $H = \frac{1}{2R_1} + \frac{1}{2R_2}$, $K = \frac{1}{R_1 R_2}$. If $R_1 = -R_2$, at every point, the surface is called minimal. This implies that K is non-positive at every point.

Chapter 3

Minimization of the functional

In order to find the local minima of the functional (2.9) we have discretized it on the cubic lattice. Thus the functional $\mathcal{F}[\phi(\mathbf{r})]$ becomes a function $F(\{\phi_{i,j,k}\})$ of N^3 variables, where $L = (N-1)h$ is the linear dimension of the cubic lattice, h is the lattice spacing, and $\{\phi_{i,j,k}\}$ stands for the set of all variables of the function. Each variable $\phi_{i,j,k}$ represents the value of the field $\phi(\mathbf{r})$ at the point $\mathbf{r} = (i,j,k)h$, and $i,j,k = 1,\ldots,N$. In our calculations we use N=129, which results in over 2 million points per unit cell.

3.1 Periodic Boundary Conditions

All structures we have investigated are periodic. Thus periodicity had to be incorporated into the functional (2.9). It was done by periodic boundary conditions:

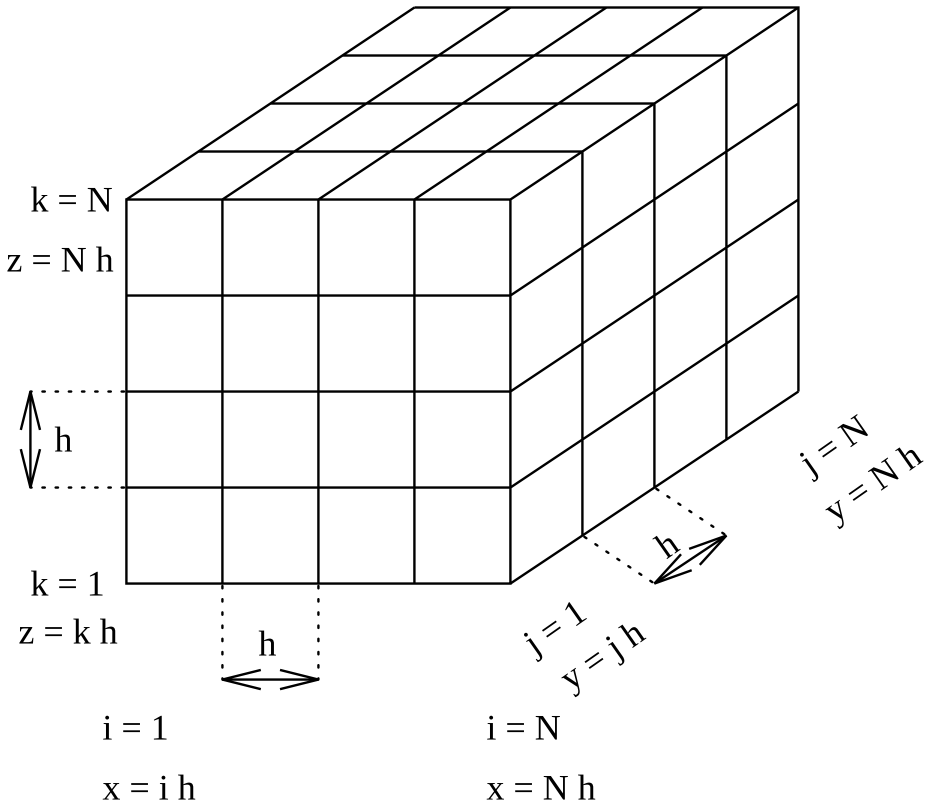

Figure 3.1: The schematic illustration of the cubic lattice used to discretize the functional (2.2). The number of lattice sites is N^3, the lattice spacing is h. The linear dimension of the lattice is $L = (N-1)h$.

$$\phi_{1,j,k} = \phi_{N,j,k} \tag{3.1}$$

$$\phi_{2,j,k} = \phi_{N+1,j,k}, \qquad \phi_{3,j,k} = \phi_{N+2,j,k} \tag{3.2}$$

$$\phi_{0,j,k} = \phi_{N-1,j,k}, \qquad \phi_{-1,j,k} = \phi_{N-2,j,k} \tag{3.3}$$

and similar in y and z directions. The points outside the unit cell, given by the periodic boundary conditions, enter the functional through the calculations of derivatives of points at the boundary and near the boundary of the lattice, i.e. when at least one of the indices i, j, k is equal to $1, 2, N-1, N$.

3.2 Discretization of derivatives

The first and second derivatives in the gradient and laplasian term of the functional (2.9) at the point $\mathbf{r} = (i, j, k)h$ on the lattice were calculated according to the following formulas [30]

$$\frac{\partial \phi(\mathbf{r})}{\partial x} \rightarrow \frac{\phi_{i+1,j,k} - \phi_{i-1,j,k}}{2h}, \tag{3.4}$$

and

$$\frac{\partial^2 \phi(\mathbf{r})}{\partial x^2} \rightarrow \frac{1}{12h^2}\Big(-\phi_{i+2,j,k} + 16\phi_{i+1,j,k} - 30\phi_{i,j,k} + 16\phi_{i-1,j,k} - \phi_{i-2,j,k} \Big), \tag{3.5}$$

and similar in y and z directions.

The mixed derivatives used in (3.15), (3.16) are calculated according to [30]

$$\frac{\partial^2\phi(\mathbf{r})}{\partial x\partial y} \rightarrow -\frac{1}{2h^2}\Bigg(\phi_{i+1,j,k} + \phi_{i-1,j,k} + \phi_{i,j+1,k} + \phi_{i,j-1,k} - 2\phi_{i,j,k} - \phi_{i+1,j+1,k} - \phi_{i-1,j-1,k}\Bigg). \tag{3.6}$$

Fig. 3.2 illustrates calculation of derivatives on the cubic lattice of: (a) first derivatives given by (3.4) , (b) second derivatives given by (3.5) , (c) mixed derivatives given by (3.6). In our calculations we used 5-point formula (3.5) to calculate the second derivatives in laplasian term in order to have more accurate approximation for small lattice size. However the 3-point formula given by [30]

$$\frac{\partial^2\phi(\mathbf{r})}{\partial x^2} \rightarrow \frac{1}{h^2}(\phi_{i+1,j,k} - 2\phi_{ijk} + \phi_{i-1,j,k}) \tag{3.7}$$

can also be used. We have compared the values for the free energy density calculated for 3-point and 5-point approximation of the second derivatives. It turned out that the values of the free energy density differed for small lattice size, $N = 9$, but for big lattice size, $N = 129$, the difference was negligible and both approximations are equally good. Moreover, the calculation of derivatives on the lattice boundary requires taking into account the points outside the lattice. These points are given by periodic boundary conditions, because we have studied periodic structures. Thus the periodicity is better

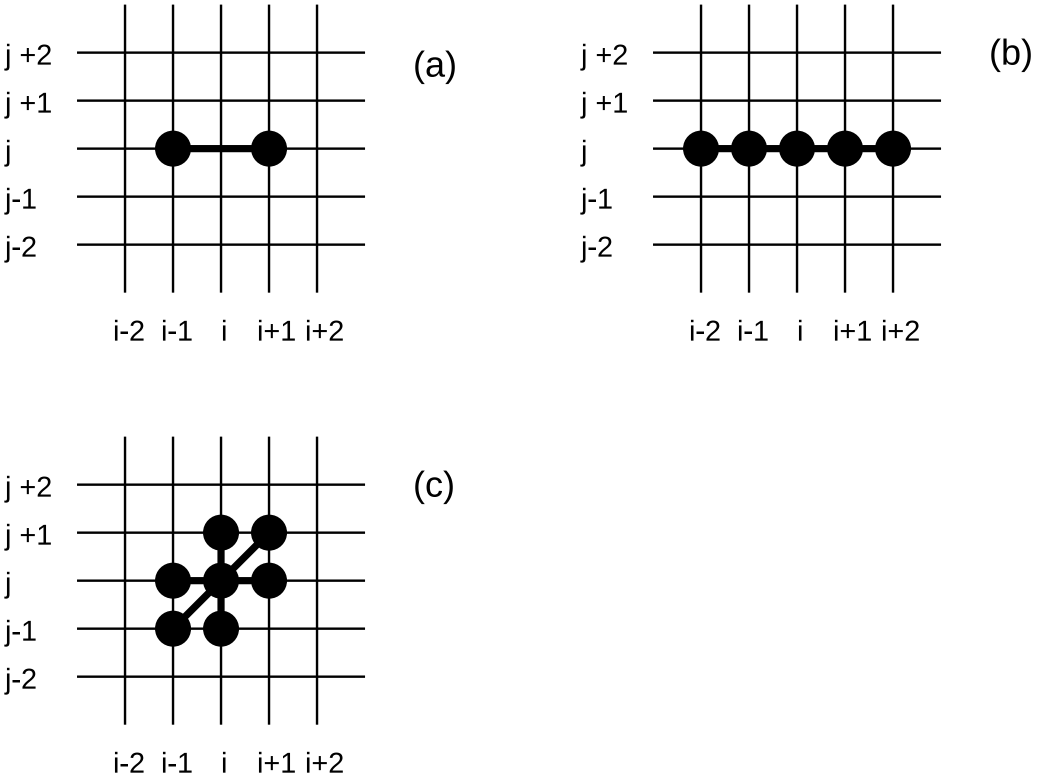

Figure 3.2: The schematic illustration of formulas used to calculate the derivatives of the discretized functional: (a) formula (3.4), (b) formula (3.5), (c) formula (3.6). The black circles show the points taken in calculation of the derivatives.

incorporated into the discretized functional by the 5-point formula, because it uses more points outside the unit cell.

3.3 Choosing the surface

The order parameter field $\phi(\mathbf{r})$ carries enormous amount of information about the local structure of the phases we have investigated. The most interesting is the topology of the phases, described by the surface

$$\phi(\mathbf{r} = (x, y, z)) = 0, \tag{3.8}$$

dividing positive and negative regions of the order parameter field. Thus it was crucial in our studies to find the location of the surface $\phi(\mathbf{r}) = 0$.

It is highly unlikely, because of numerical accuracy, that a value of the field $\phi(\mathbf{r}) = \phi_{i,j,k}$ at the point $\mathbf{r} = (i, j, k)h$ on the lattice is exactly zero. Therefore the points of the surface have to be localized by interpolation between the neighboring sites of the lattice. If $\phi(\mathbf{r}_1 = (i, j, k)h) = \phi_{i,j,k} < 0$ and $\phi(\mathbf{r}_2 = (i+1, j, k)h) = \phi_{i+1,j,k} > 0$ then the point $\mathbf{r}_0$, for which $\phi(\mathbf{r}_0) = 0$, must lie between the points $\mathbf{r}_1 = (i, j, k)h$ and $\mathbf{r}_2 = (i + 1, j, k)h$. Moreover, the location of $\mathbf{r}_0$ depends on the values of the field at the points $\mathbf{r}_1$ and $\mathbf{r}_2$ in the following way

$$\mathbf{r}_0 = \left(i + \frac{|\phi_{i,j,k}|}{|\phi_{i,j,k} - \phi_{i+1,j,k}|}, j, k \right) h. \tag{3.9}$$

This approximation is legible because the field $\phi(\mathbf{r})$ is very smooth. Fig. 3.3

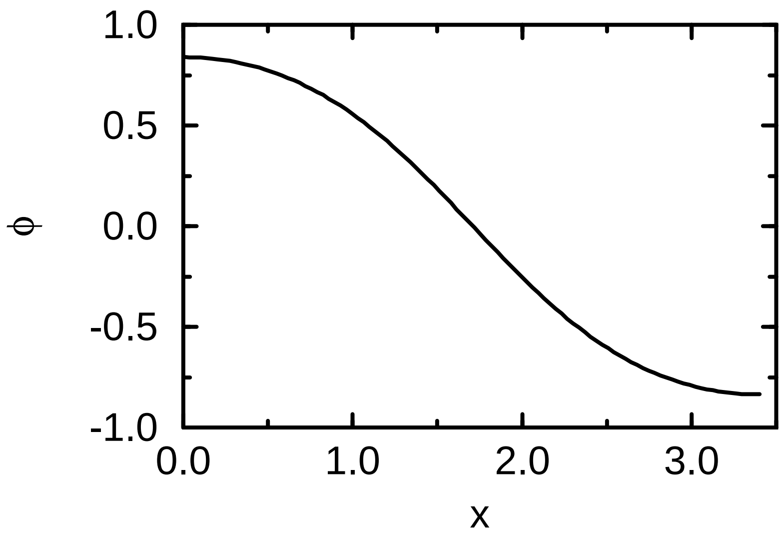

Figure 3.3: The order parameter profile $\phi(x)$ for the lamellar phase, calculated from the functional (2.9) for the parameters $f_0 = 0$ and $g_0 = 0$. Half of the unit cell is presented. Here $N = 400$, thus, h, the distance between the lattice size is $3.4/400 = 0.0085$. Certainly this justifies the linear interpolation.

shows the profile of the order parameter $\phi(x)$ for the lamellar phase. In the vicinity of $\phi(x) = 0$ the profile is almost a straight line. Thus for small values of lattice spacing, h, finding the points of the surface $\phi(\mathbf{r}) = 0$ should not introduce significant errors. As our calculations show it is done with high accuracy.

3.4 Triangulation, Surface Area, Volume

In the way described in the preceding section one can find the points of the surface $\phi(\mathbf{r}) = 0$ located between the neighboring lattice sites. However this is not enough to describe the surface. It is also necessary to specify the connections between these points to characterize the surface.

Due to discretization the unit cell is divided on $(N-1)^3$ small cubes of the size of lattice spacing, h. The surface $\phi(\mathbf{r}) = 0$ passing through a small cube cuts out of it a polygon, which edges are formed by intersection of the surface and faces of the small cube. The edges of the polygon can be approximated by straight lines. The possible configurations of the surface $\phi(\mathbf{r}) = 0$ cutting a small cube are pictured in Fig. 3.4. The surface $\phi(\mathbf{r}) = 0$ can cut out only four kinds of polygons: a triangle, a tetragon, a pentagon, a hexagon. The edges of these polygons except a triangle do not lie in a common plane. It is necessary to specify also the connections between the vertices of the polygon, to characterize the surface unambiguously. It was done in the way shown in Fig. 3.4 with thick dotted lines in the patches of the surface inside the small cubes. This procedure makes the surface covered only with triangles. The triangulation described above was used to calculate the surface area inside a unit cell by summing up the surface area of all triangles.

The triangulation was also used to calculate the volume ratio of the two subvolumes.The surface $\phi(\mathbf{r}) = 0$ separates the volume of a given phase into two subvolumes, first occupied by the field $\phi(\mathbf{r}) > 0$ and second by $\phi(\mathbf{r}) < 0$. In order to calculate the volume occupied by the negative or

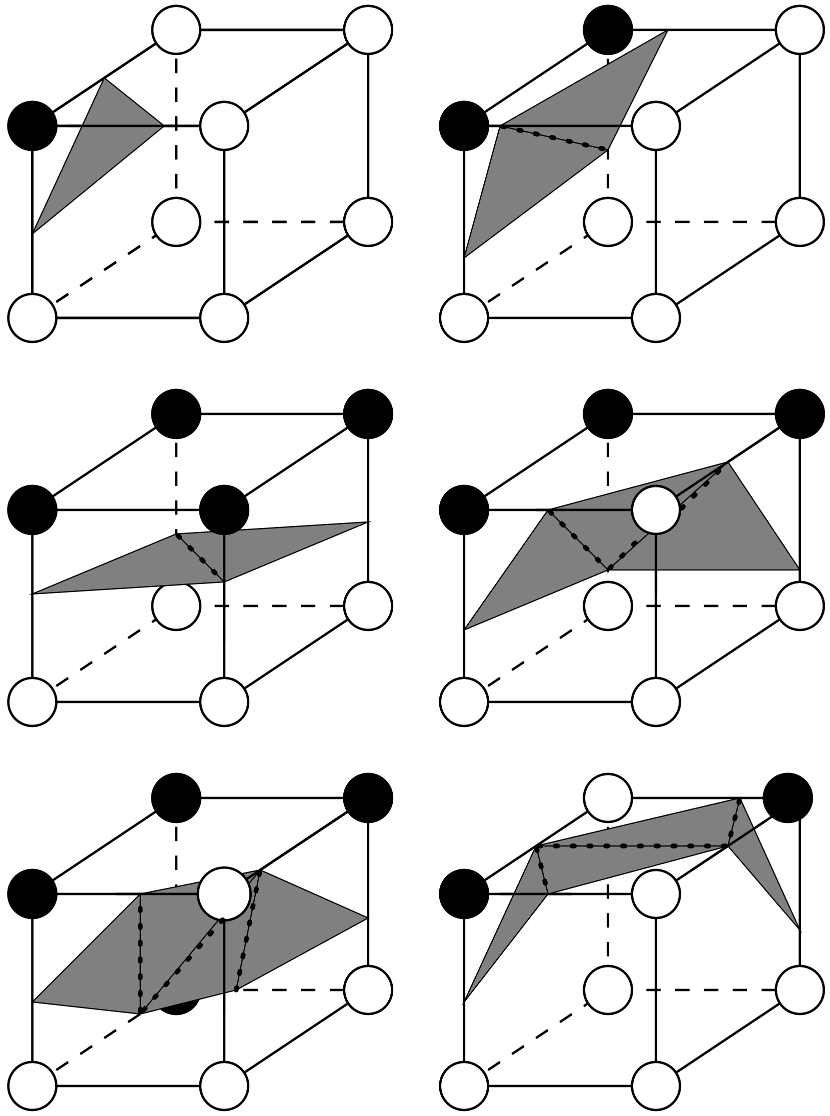

Figure 3.4: The possible configurations of passing the surface $\phi(\mathbf{r}) = 0$ through the field $\phi(\mathbf{r})$ discretized on the lattice. Black circles represent $\phi_{i,j,k} < 0$, whereas white circles $\phi_{i,j,k} > 0$. The cubes represent the smallest pieces, of the lattice of the linear dimension, h.

positive values of the field $\phi(\mathbf{r})$ the volume of the small cubes not cut by the surface $\phi(\mathbf{r}) = 0$ is calculated. Next we use the triangulated surface $\phi(\mathbf{r}) = 0$ to divide the small cubes with the values of the field $\phi(\mathbf{r})$ of different sign at the vertices. The surface $\phi(\mathbf{r}) = 0$ divides a small cubes into two polyhedra. The volumes of these polyhedra for negative and positive values of the field $\phi(\mathbf{r})$ was calculated and added to the previously calculated volume for regions of positive and negative values of $\phi(\mathbf{r})$.

For more than one periodic surface, in the unit cell, it is necessary to separate different surfaces to be able to calculate surface area and genus of each surface. In order to find the points which belong to the same surface one has to chose an arbitrary point on one of the surfaces and following the connections between points find the rest of the points belonging to this surface. The set of connections will uniquely specify the surface. Fig. 3.5 illustrates the way this process can be done for two surfaces. Having chosen an arbitrary point on one surface, represented by a black circle in Fig. 3.5a, one has to find among all the connections between couples of points specified by the triangulation, the connections including this point. They are represented by thick solid lines connecting the black circle with the white circles. Next one has to chose arbitrarily a point among the points represented by white circles and find all connections between this point and the points remaining after removing from the set of connections the connections containing the first point. This is shown in Fig 3.5b. Such procedure has to be repeated until no more than one point represented by the white circle is left.

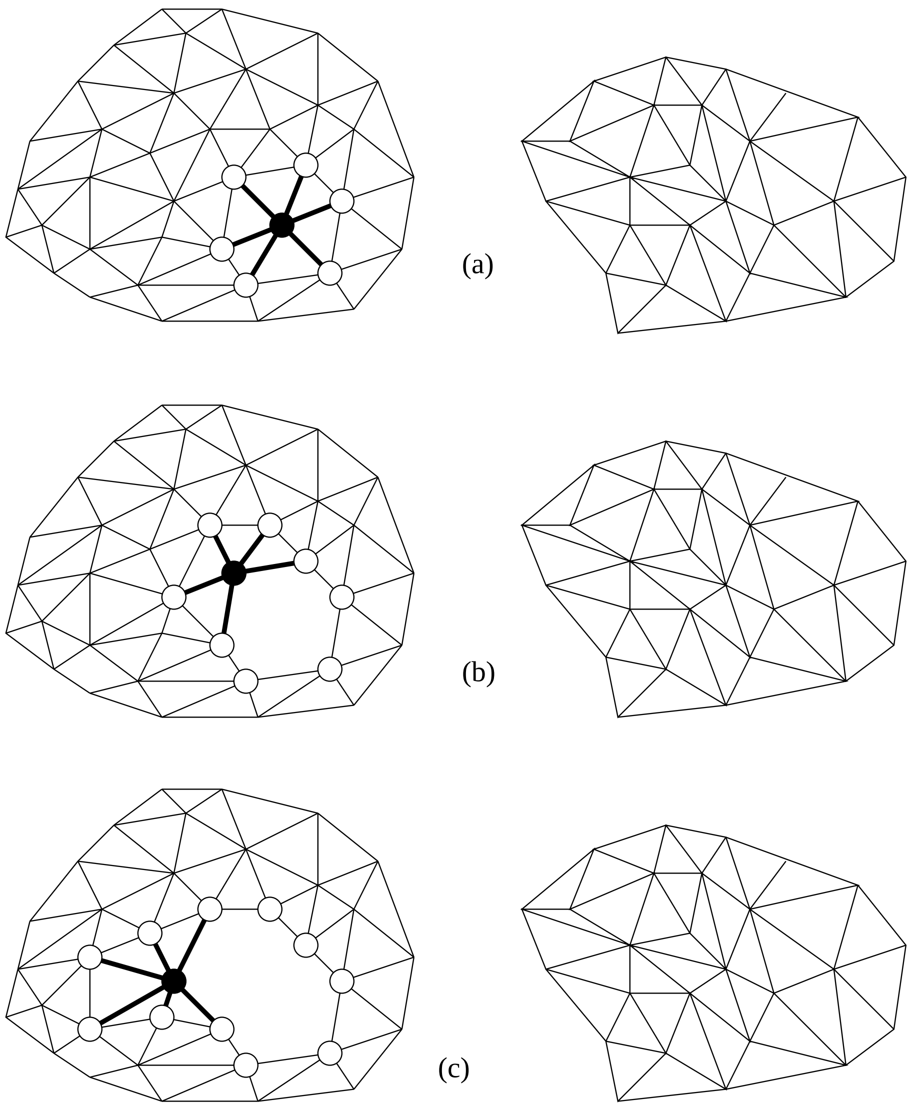

Figure 3.5: The schematic illustration of the separation of two disjoint surfaces.

3.5 Euler characteristics, genus

The triangulation can also be used to calculate the Euler characteristics, χ, of the surface inside the unit cell. The calculation of χ can be done according to the Euler formula [31]

$$\chi = F + V - E, \tag{3.10}$$

where F,V,E is the number of faces (F), vertices (V), and edges (E) of the polygons cut out by the surface $\phi(\mathbf{r}) = 0$ in the small cubes of dimension of lattice spacing, (Fig. 3.5). The fact that each polygon is inside a small cube makes the calculation very easy, because each vertex of the polygon belongs to four polygons since it lies in the edge of the small cube. Therefore to calculate χ one does not need to know the connections between points. It is sufficient to know only how many times the surface $\phi(\mathbf{r}) = 0$ cuts the edges of the small cube and how many cubes it cuts. The number of faces (F) is therefore the number of small cubes cut by the surface $\phi(\mathbf{r}) = 0$, that is the cubes with the values of the field $\phi(\mathbf{r}) = \phi_{i,j,k}$ of different sign at its vertices. The number of vertices is given by the number of intersections of the surface $\phi(\mathbf{r}) = 0$ with the edges of the small cubs taken with a weight $1/4$, because each edge belongs to four cubes. The number of edges (E) is the same as the number of vertices, but it has to be taken with a weight $1/2$ because the polygon edges lie in the faces of small cubes and each face belongs to two cubes.

The Euler characteristic for the closed surface is related to the Gaussian (K) curvature and genus (g) of this surface in the following way [31, 32]

$$\chi = \frac{1}{2\pi}\int_S K dS = 2(1-g), \tag{3.11}$$

where the integral is taken over the surface S. Genus is an integer number and tells how many holes are in a closed surface. For example the genus for a sphere is zero, for a torus is one and for a pretzel is two. The structures we have investigated are infinite and periodic. The genus for an infinite surfaces is infinite, of course, but for a finite piece of this surface, in a unite cell, is finite and characterize the surface. Due to periodicity the unit cubic cell can be treated as a closed surface in four dimensions making calculation of genus for the infinite periodic surface fully justified [33]. Therefore the genera of the structures were calculated according to: $g = 1 - \chi/2$, where χ was the Euler characteristics for the surface inside a unit cell.

3.6 Curvatures

The Gaussian and the mean curvatures present another characteristics of the internal surfaces given by $\phi(\mathbf{r}) = 0$. In the description of the model we have mentioned that some of the structures in the model should be characterized by zero mean curvature at every point of the internal interface. Here we present the method used to compute Gaussian and mean curvatures. The unit normal $\mathbf{n}(\mathbf{r})$ at the point $\mathbf{r}$ is given by the gradient of the field $\phi(\mathbf{r})$:

$$\mathbf{n}(\mathbf{r}) = \frac{\nabla\phi(\mathbf{r})}{\mid \nabla\phi(\mathbf{r}) \mid}. \tag{3.12}$$

The mean (H) curvatures is given by the divergence of the unit vector [34], normal to the surface at the point $\mathbf{r}$, $\mathbf{n}(\mathbf{r})$

$$H(\mathbf{r}) = -\frac{1}{2}\nabla\mathbf{n}(\mathbf{r}) = -\frac{1}{2}\nabla\frac{\nabla\phi(\mathbf{r})}{\mid \nabla\phi(\mathbf{r}) \mid}. \tag{3.13}$$

and the Gaussian curvature (K) by the formula [35]

$$K(\mathbf{r}) = \frac{1}{2}(-(\partial_i n_j)^2 + (\nabla\mathbf{n}(\mathbf{r}))^2). \tag{3.14}$$

In numerical calculations of the curvatures we used the following formulas [34, 36]:

$$H = -\frac{1}{2\sqrt{\phi_x^2 + \phi_y^2 + \phi_z^2}}\frac{B}{A} \tag{3.15}$$

$$K = \frac{1}{\phi_x^2 + \phi_y^2 + \phi_z^2}\frac{C}{A} \tag{3.16}$$

where A, B , and C are obtained from:

$$det \begin{pmatrix} (\phi_{xx}-\lambda) & \phi_{xy} & \phi_{xz} & \phi_x \\ \phi_{yx} & (\phi_{yy}-\lambda) & \phi_{yz} & \phi_y \\ \phi_{zx} & \phi_{zy} & (\phi_{zz}-\lambda) & \phi_z \\ \phi_x & \phi_y & \phi_z & 0 \end{pmatrix} = A\lambda^2 + B\lambda + C \tag{3.17}$$

and are given by:

$$A = -\left(\phi_x^2 + \phi_y^2 + \phi_z^2\right) \tag{3.18}$$

$$\begin{aligned} B = {} & \phi_x^2\left(\phi_{yy}+\phi_{zz}\right) + \phi_y^2\left(\phi_{xx}+\phi_{zz}\right) + \phi_z^2\left(\phi_{xx}+\phi_{yy}\right) \\ & - 2\phi_x\phi_y\phi_{xy} - 2\phi_x\phi_z\phi_{xz} - -2\phi_y\phi_z\phi_{yz} \end{aligned} \tag{3.19}$$

$$\begin{aligned} C = {} & \phi_x^2(\phi_{yz}^2 - \phi_{yy}\phi_{zz}) + \phi_y^2(\phi_{xz}^2 - \phi_{xx}\phi_{zz}) + \phi_z^2(\phi_{xy}^2 - \phi_{xx}\phi_{yy}) \\ & + 2\phi_x\phi_z(\phi_{xz}\phi_{yy} - \phi_{xy}\phi_{yz}) + 2\phi_x\phi_y(\phi_{xy}\phi_{zz} - \phi_{xz}\phi_{yz}) \\ & + 2\phi_y\phi_z(\phi_{yz}\phi_{xx} - \phi_{xy}\phi_{xz}) \end{aligned} \tag{3.20}$$

The mean and Gaussian curvatures have to be computed at the points of the surface $\phi(\mathbf{r}) = 0$. These points do not lie exactly at the lattice sites. In order to calculate the derivatives of the field $\phi(\mathbf{r})$ at the point $\mathbf{r}_0$, for which $\phi(\mathbf{r_0}) = 0$, according to the formulas (3.4), (3.5), (3.6) the values of the field $\phi(\mathbf{r})$ at the points $\mathbf{r}_0 + (0,0,h)$, $\mathbf{r}_0 + (0,h,0)$, $\mathbf{r}_0 + (h,0,0)$, $\mathbf{r}_0 + (0,0,2h)$,

$\mathbf{r}_0 + (0, 2h, 0)$, $\mathbf{r}_0 + (2h, 0, 0)$, $\mathbf{r}_0 + (0, h, h)$, $\mathbf{r}_0 + (h, h, 0)$, $\mathbf{r}_0 + (h, 0, h)$ have to be interpolated. The way the interpolation is done is shown in Fig. 3.6. The

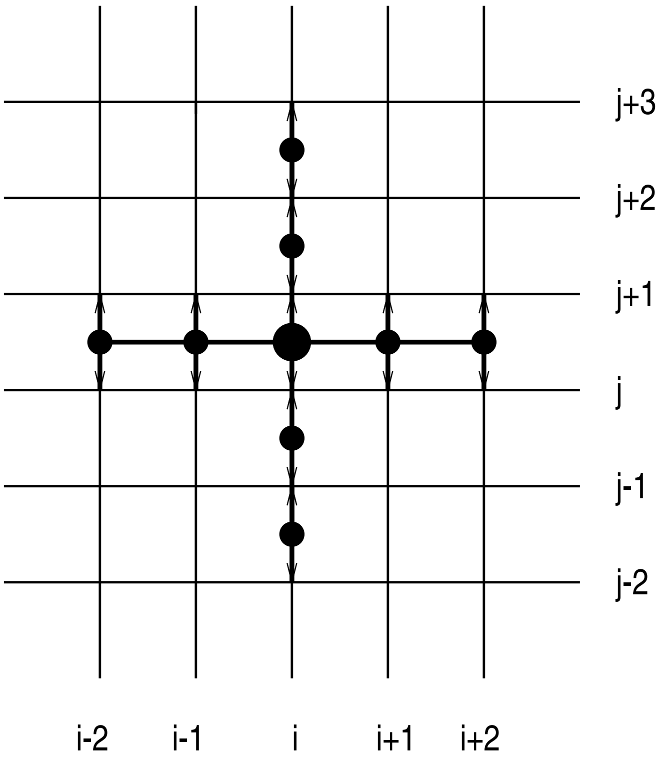

Figure 3.6: The way of interpolation of derivatives of the field $\phi(\mathbf{r})$ at the surface $\phi(\mathbf{r}) = 0$. The big black circle represents the point on the surface $\phi(\mathbf{r}) = 0$, the smaller black circles represent the points taken in calculations of derivatives. The arrows show the points on the lattice taken to interpolate the points between the lattice sites.

big black circle represents the point $\mathbf{r_0}$. The smaller black circles represent the points taken to calculate the derivatives. The values of the field in these points are interpolated from the values of the field at the nearest sites of the lattice indicated by the arrows. The point $\mathbf{r_0}$ is $\frac{|\phi_{i,j,k}|}{|\phi_{i,j,k}-\phi_{i,j+1,k}|} = \Delta h$ away from the point $\mathbf{r} = (i,j,k)h$. Then the value of the field $\phi(\mathbf{r})$ at e.g. the point $\mathbf{r}_0 + (0,h,0)$ is $\Delta h(\phi_{i,j+1,k} - \phi_{i,j,k})$. The values of the field $\phi(\mathbf{r})$ in the remaining points can be calculated in a similar way.

It is remarkable that the properties characterizing two dimensional surface can be inferred from the three dimensional field.

3.7 Building initial configuration

The minimization procedure always requires an initial configuration. Here we present the initial configurations used in minimization of structures of different symmetries.

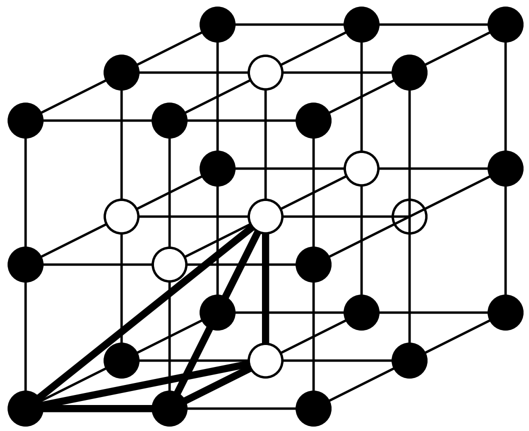

Figure 3.7: The initial configuration used to create structures of symmetry of simple cubic phase

The initial configuration is set up by building the field $\phi(\mathbf{r})$ for a unit cell

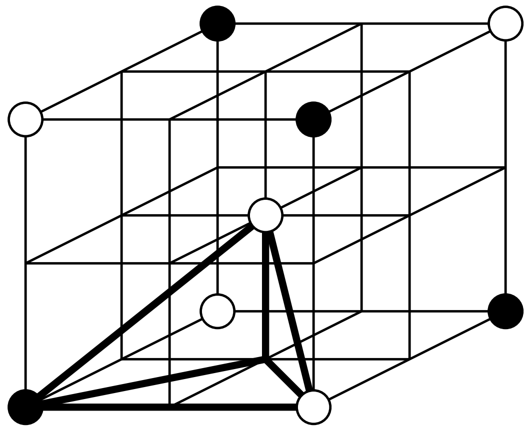

Figure 3.8: The initial configuration used to create structures of symmetry of double diamond phase

first on a small cubic lattice, $N = 3$ or 5, analogically to a two component, AB, molecular crystal. The value of the field $\phi(\mathbf{r}) = \phi_{i,j,k}$ at the point $\mathbf{r} = (i, j, k)h$ on the lattice is set to 1 if in the molecular crystal an atom A is in this place, if there is an atom B $\phi_{i,j,k}$ is set to -1, if there is an empty place $\phi_{i,j,k}$ is set to 0. Fig. 3.7 shows the initial configuration used to build the field $\phi(\mathbf{r})$ for the simple cubic phase unit cell. Filled black circles represent atoms of type A and hollow circles represent atoms of type B. In this case all sites are occupied by atoms A or B. Fig. 3.8 shows the initial configuration used to build the field $\phi(\mathbf{r})$ for the double diamond phase in 1/8 of the unit cell. There are unoccupied sites in this case and in these sites the value of the field $\phi(\mathbf{r}) = \phi_{i,j,k}$ is set to zero. It would be difficult to present the initial configuration for the gyroid phase, because it would require drawing the picture of lattice of size $N = 9$. Such a picture would be unreadable.

Therefore we present this configuration schematically in Fig. 3.9. The solid and dotted lines show the channels of oil and water. The thick dashed lines show the region occupied by rectangular parallelopiped used to build the unit cell. The fractions represent the value of z coordinate of an atom in the unit cell. In order to better visualize this configuration we present in Fig. 3.10 the points on the lattice, in a unit cell, with the values of the field $\phi(\mathbf{r})$ set initially to -1 (light grey spheres) and +1 (dark grey spheres).

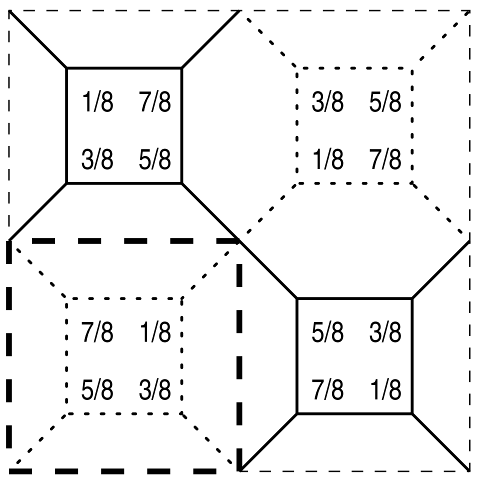

Figure 3.9: The schematic representation of the initial configuration used to create structures of symmetry of gyroid phase.

The tetrahedrons drawn in Fig. 3.7 and Fig. 3.8 with thick solid lines are the kaleidoscopic cells used to build the unit cell. The way of constructing the unit cell by replicating the kaleidoscopic cell is described in Section 3.8. One can easily see now, that in order to build the field in a unit cell on a small cubic lattice, $N = 3$, it is enough to specify the values of the field

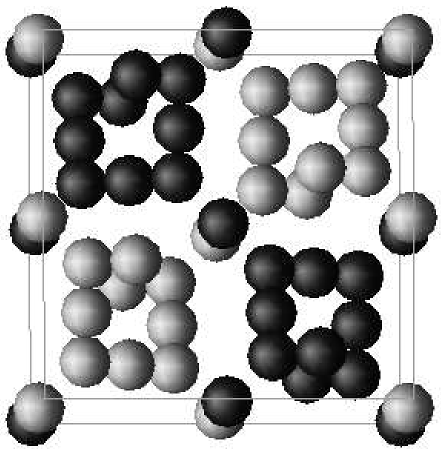

Figure 3.10: The initial configuration used to create structures of symmetry of gyroid phase.

$\phi(\mathbf{r}) = \phi_{i,j,k}$ only at the points inside the tetrahedrons. The values of the field at the remaining points can be set by using the symmetry of the structures. Thus instead of specifying $3^3 = 27$ values of $\phi_{i,j,k}$ one has to specify these values at four point of the cubic lattice for the simple cubic structure. Using this method in the case of double diamond structures gives even bigger gain, where it is sufficient to set the values of the field at five points in order to set up the field for a cubic lattice containing $5^3 = 125$ points.

The small lattice can be enlarged to desired size by changing the number of points from N to $2N - 1$ and finding the values of $\phi_{i,j,k}$ in new lattice sites by interpolation. Fig. 3.11 illustrates how the interpolation can be done. The hollow circles represent the values of the lattice mapped to the enlarged lattice. The values on the edges of the cube, represented by black

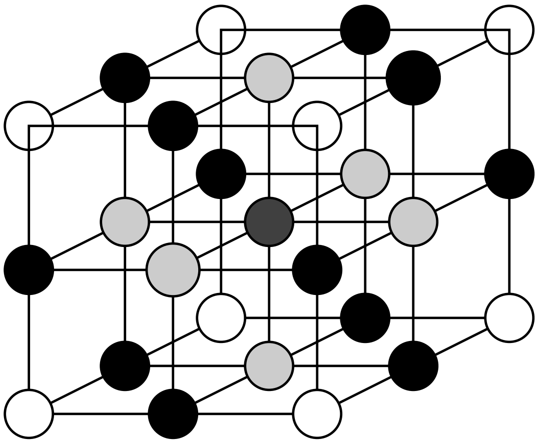

Figure 3.11: The illustration of interpolation done during enlarging the lattice size.

circles, are calculated by taking 1/2 of the sum of the values on vertices of the cube common with these edges. The values at the center of faces of the cube, represented by light grey circles, are computed as 1/4 of the sum of the values at the edges common with these faces. The value at the center of the cube is calculated as 1/6 of the sum of the values at the centers of the cube faces. There are of course other possibilities of doing the interpolation. The interpolation done to enlarge the lattice has no influence on the results. It may only speed up the calculations if it is done appropriately.

3.8 Symmetry

We impose on the field $\phi(\mathbf{r})$ the symmetry of the structure we are looking for by building up the field inside a unit cubic cell of a smaller polyhedron, replicating it by reflections, translations, and rotations. These polyhedra are pictured with thick solid lines in Figs. 3.12, 3.14, 3.13. They are identical with the polyhedra described by Coxeter [37] as kaleidoscopic cells. Such a procedure not only guarantees that the field has required symmetry but also enables substantial reduction of independent variables $\phi_{i,j,k}$ in the function $F(\{\phi_{i,j,k}\})$.

The structures we have generated can be, in principle, characterized by space group symmetry [38, 39, 32] analogically to molecular crystals. The simple cubic structure has the space group $Im\bar{3}m$, double diamond $F\bar{4}3m$, gyroid $Ia\bar{3}d$. However this is not always obvious even for the structures of simple topology which Bravais lattice should be assign to a given structure [32]. For more complex structures assigning a Bravais lattice becomes not clear. Therefore we decided to characterize the symmetry of the structures, we have generated, by including it in the class of symmetry characteristic for the following structures: simple cubic, double diamond, and gyroid. All these structures belong to the class of cubic symmetry, thus here we generate only the structures belonging to this class.

The structures having the symmetry of the simple cubic phase are built of quadrirectangular tetrahedron replicating it by reflection, Fig. 3.12. The faces of the tetrahedron lie in the planes of mirror symmetry. The volume of the tetrahedron is $1/48$ of the unit cell volume.

The structures of the double diamond phase symmetry are built in the following way. First the unit cell is divided into eight smaller cubes. The field in the one of the small cubes is built of trirectangular tetrahedron in the same

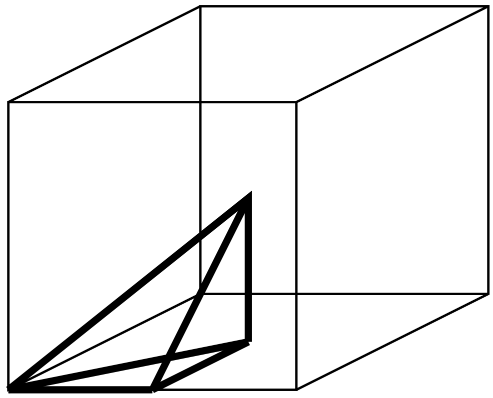

Figure 3.12: The thin solid lines show the unit cell. The thick solid lines show the kaleidoscopic cell used to create structures of simple cubic phase symmetry: the quadrirectangular tetrahedron. See Fig. 3.7.

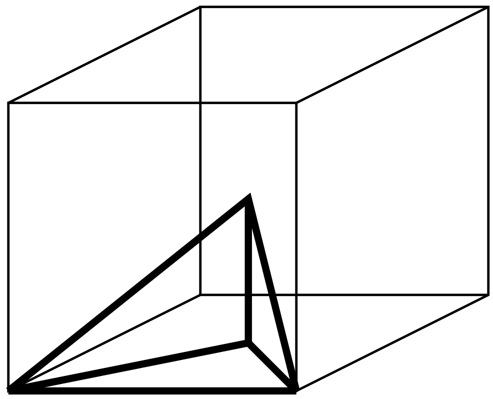

Figure 3.13: The thin solid lines show 1/8 of the unit cell. The thick solid lines show the kaleidoscopic cell used to create structures of double diamond phase symmetry: trirectangular tetrahedron. See Fig. 3.8.

way as in the previous case, Fig. 3.13. The volume of the tetrahedron is $1/24$ of the unit cell volume. Next the field in the unit cell is build of this cube by translations and translations combined with a change of sign of the field from $\phi_{i,j,k}$ to $-\phi_{i,j,k}$. The cube with the field build of the tetrahedron is translated by the following vectors: $[L/2, L/2, 0]$, $[0, L/2, L/2]$, and $[L/2, 0, L/2]$. Next the sign of the field in the small cube is changed and the cube with such a different field is translated by the following vectors: $[0, 0, L/2]$, $[0, L/2, 0]$, $[L/2, 0, 0]$, and $[L/2, L/2, L/2]$. L in both cases is the unit cell length. Such a procedure enables reduction of the unit cell volume by a factor $1/(8*24) = 1/192$.

If the $\phi(\mathbf{r})$,$-\phi(\mathbf{r})$ symmetry is not applied the trirectangular tetrahedron can also be used to create the structures of double diamond phase symmetry. In such a case the cube shown in Fig. 3.13 as $1/8$ of the unit cell becomes the unit cell. The unit cell volume is therefore reduced by the factor $1/24$.

The structures of gyroid phase symmetry are built of rectangular parallelopiped, Fig. 3.14. It consists $1/16$ of the unit cell volume. The parallelopiped is rotated by 90 degrees according to four fold screw rotation axis parallel to z direction, located at the point $\mathbf{r} = (L/4, L/4, L/4)$ and translated in the direction of z axis by the vector $[L/4, 0, 0]$. Repeating this operation three times fills out $1/4$ of the unit cell volume with a new rectangular parallelopiped spanned by a vector $[L, L/2, L/2]$ located at the point $\mathbf{r} = (0, 0, 0)$. Next this new parallelopiped is rotated according to two fold rotation axis parallel to y direction and located at the point $\mathbf{r} = (L/2, 0, L/2)$. The parallelopiped created by this operation spanned by the vector $[L, L/2, L/2]$ located at the

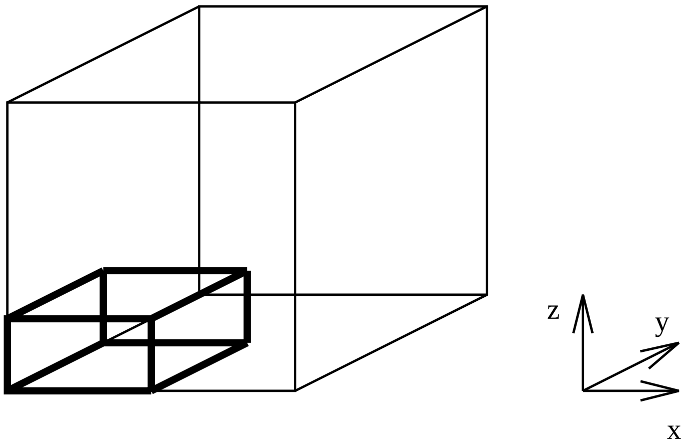

Figure 3.14: The thin solid lines show the unit cell. The thick solid lines show the kaleidoscopic cell used to create structures of gyroid phase symmetry: the parallelepiped. See Figs. 3.9, 3.10.

point $\mathbf{r} = (L/2, 0, 0)$ is translated by the vector $[-L/2, L/2, 0]$. The sign of the field in this parallelopiped is changed from $\phi_{i,j,k}$ to $-\phi_{i,j,k}$. After these transformation 1/2 of the unit cell is recreated. The other half of the unit cell is created of the previous one by rotating it according to two fold rotation axis parallel to z direction and located at the point $\mathbf{r} = (L/2, L/2, 0)$.

3.9 Conjugate gradient method

We use conjugate gradient method [40] to minimize the function $F(\{\phi_{i,j,k}\})$. Minimization was done with respect to $\{\phi_{i,j,k}\}$ for a given value of the cell length $L = (N-1)h$. We have varied h to find the cell length for the lowest value of the free energy functional $F(\{\phi_{i,j,k}\})$. First we have done the calculation for a small lattice size $N = 33$. The configuration obtained for the lattice size N was next used to produce the configuration for the bigger lattice size $2N-1$. It was done by interpolation the values of the field $\phi(\mathbf{r}) = \phi_{i,j,k}$ from the small lattice to fill out the empty sites on the bigger lattice in the way described in Section 3.7.

The conjugate gradient method requires calculation of partial derivatives of the function $F(\{\phi_{i,j,k}\})$

$$\frac{\partial F(\{\phi_{l,m,n}\}, \phi_{l_1,m_1,n_1})}{\partial \phi_{l_1,m_1,n_1}} \tag{3.21}$$

where $\{\phi_{l,m,n}\}$ is the set of all variables of the function $F[\{\phi_{i,j,k}\}]$ except the variable ϕ_{l_1,m_1,n_1}. This derivative can be, in principle, calculated analytically. However, due to reduction of the unit cell volume (see for example Figs. 3.12, 3.13) these derivatives would have to be computed in a different way in different places of this volume, therefore the analytical calculation of the derivatives would require different formulas for these derivatives at the vertives, edges and faces. The analytical calculation of derivatives would also introduce some inconsistency to our calculations, because we calculate all other derivatives numerically. Fortunately, it does not imply the loss of accuracy, therefore the derivatives (3.21) are approximated in our calculations by

$$\frac{F(\{\phi_{l,m,n}\}, \phi_{l_1,m_1,n_1} + \Delta\phi) - F(\{\phi_{l,m,n}\}, \phi_{l_1,m_1,n_1})}{\Delta\phi} \tag{3.22}$$

where $\Delta\phi << \phi_{i,j,k}$. It is extremally important to code this part of the program efficiently. It may result in speeding up the program by few orders of magnitude if the number of variables $\phi_{i,j,k}$ is large. It is worth to note that the value of the expression (3.22) depends only on the values of ϕ_{l_1,m_1,n_1} its near neighbors and next near neighbors. Thus instead of calculating the values of the function $F(\{\phi_{i,j,k}\})$ in all lattice points it is sufficient to calculate these values only in a few points.

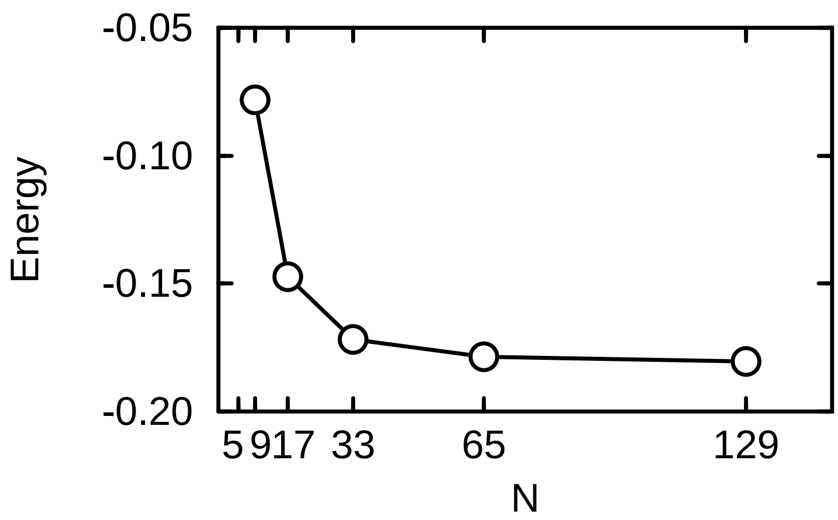

Figure 3.15: The free energy per unit volume for the simple cubic structure, calculated from the functional (2.9) for the parameters $f_0 = 0$ and $g_0 = 0$ as a function of the lattice size.

The solution for the discretized model of a continuous functional is obtained with certain accuracy. The accuracy depends on the value of the

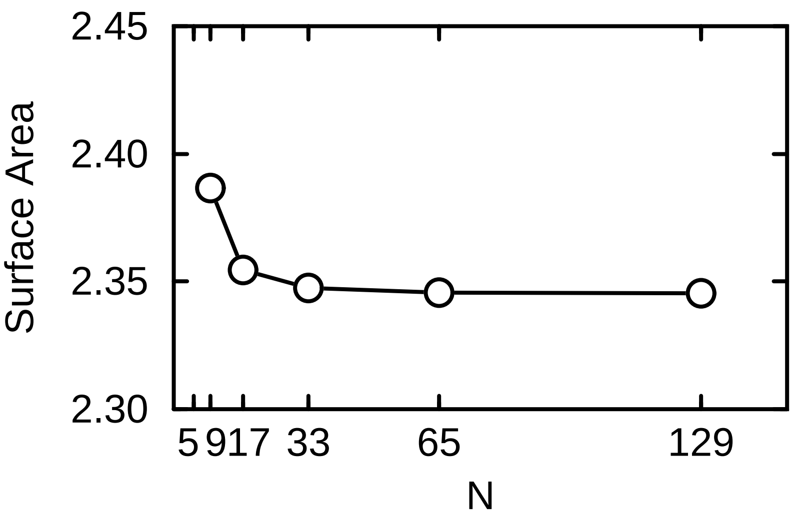

Figure 3.16: The normalized surface area per face of the unit cell of $\phi(\mathbf{r}) = 0$ for the simple cubic structure, calculated from the functional (2.9) for the parameters $f_0 = 0$ and $g_0 = 0$ as a function of the lattice size.

lattice spacing h and the number of points N. We have checked the accuracy of our results by calculating the free energy and the surface area of $\phi(\mathbf{r}) = 0$ for a few different sizes of the lattice. Fig. 3.15 shows that the free energy is very sensitive for the lattice size. We used in our calculations $N = 129$ which results in over 2 million points per unit cell. This value seems to give sufficient accuracy for the calculation of the free energy. For the calculation of the surface area of $\phi(\mathbf{r}) = 0$ smaller lattice can be used to obtain high accuracy. Fig. 3.16 shows that the values of the surface area of the internal interface change only slightly for $N = 33, 65, 129$.